

# Computational Methods for Ideal Magnetohydrodynamics

Andrew Kercher

A defense of the dissertation submitted in partial fulfillment of the requirements  
for the degree of Doctor of Philosophy  
George Mason University

25 August 2014

# Introduction

- Compound wave formation in MHD bow shock simulations.

# Introduction

- Compound wave formation in MHD bow shock simulations.
- Compound wave product of numerical diffusion.

# Introduction

- Compound wave formation in MHD bow shock simulations.
- Compound wave product of numerical diffusion.
- Slow convergence with finite volume schemes.

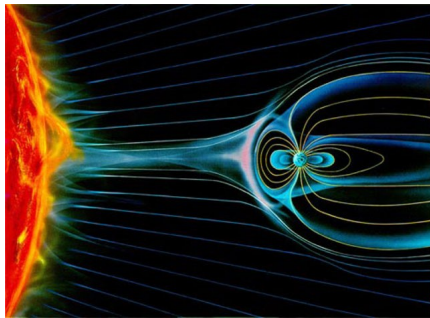
# Introduction

- Compound wave formation in MHD bow shock simulations.
- Compound wave product of numerical diffusion.
- Slow convergence with finite volume schemes.
- Compound wave modification (CWM).
  - ▶ Modification to the HLLD approximate Riemann solver.
  - ▶ Removes compound wave, correctly computes rotational discontinuity.
  - ▶ Converges at all grid resolutions.
  - ▶ FAST! HLLD intermediate states are already calculated.

# Introduction

- Compound wave formation in MHD bow shock simulations.
- Compound wave product of numerical diffusion.
- Slow convergence with finite volume schemes.
- Compound wave modification (CWM).
  - ▶ Modification to the HLLD approximate Riemann solver.
  - ▶ Removes compound wave, correctly computes rotational discontinuity.
  - ▶ Converges at all grid resolutions.
  - ▶ FAST! HLLD intermediate states are already calculated.
- Description multi-dimensional fluid solver capable of shared memory parallelism.
  - ▶ Hydrodynamics and ideal MHD.
  - ▶ Algorithms implemented for unstructured grids.

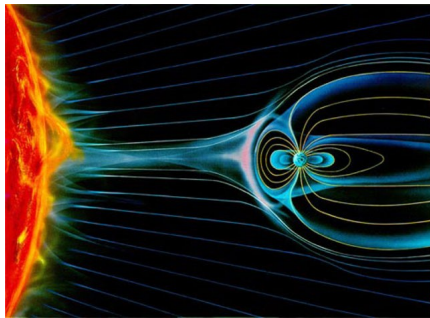
# Space Weather



Source [10]

- Sun-earth interaction:
  - ▶ Super-sonic plasma originating at sun travels toward earth.

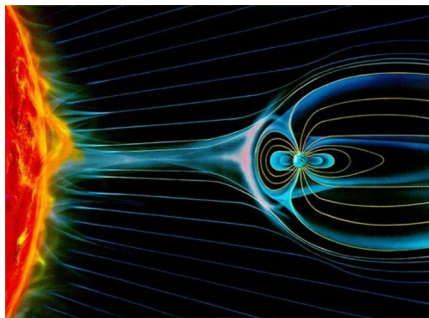
# Space Weather



Source [10]

- Sun-earth interaction:
  - ▶ Super-sonic plasma originating at sun travels toward earth.
  - ▶ Slowed down by magnetic field of Earth.

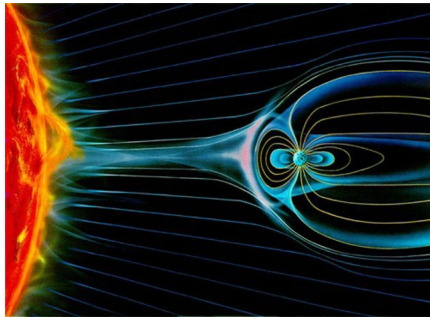
# Space Weather



Source [10]

- Sun-earth interaction:
  - ▶ Super-sonic plasma originating at sun travels toward earth.
  - ▶ Slowed down by magnetic field of Earth.
  - ▶ Plasma flow becomes subsonic forming the bow shock.

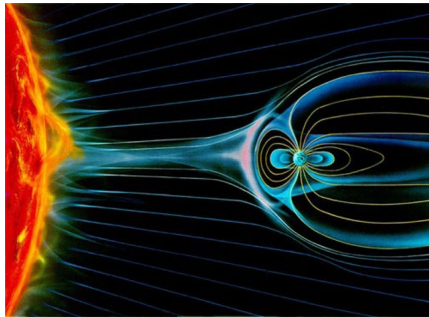
# Space Weather



Source [10]

- 2D ideal MHD bow shock simulation. [2]
  - ▶ Results contained intermediate shocks.

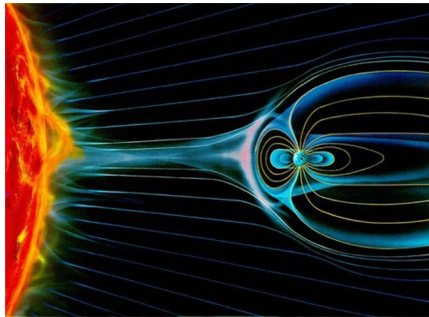
# Space Weather



Source [10]

- 2D ideal MHD bow shock simulation. [2]
  - ▶ Results contained intermediate shocks.
  - ▶ Intermediate shocks considered inadmissible in ideal MHD [7]

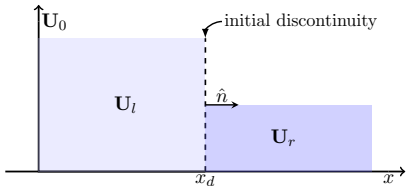
# Space Weather



Source [10]

- 2D ideal MHD bow shock simulation. [2]
  - ▶ Results contained intermediate shocks.
  - ▶ Intermediate shocks considered inadmissible in ideal MHD [7]
  - ▶ Cause?

# Riemann Problems

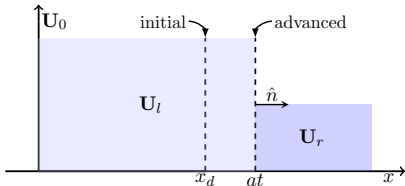


$$\frac{\partial \mathbf{U}}{\partial t} + \frac{\partial \mathbf{F}}{\partial \mathbf{x}} = \mathbf{0},$$

$$\mathbf{U}_0 = \begin{cases} \mathbf{U}_l & \text{if } x < x_d, \\ \mathbf{U}_r & \text{if } x > x_d, \end{cases}$$

- Initial discontinuity at  $x_d$  separates two constant states.

# Riemann Problems



$$\frac{\partial \mathbf{U}}{\partial t} + \frac{\partial \mathbf{F}}{\partial \mathbf{x}} = \mathbf{0},$$

$$\mathbf{U}_0 = \begin{cases} \mathbf{U}_l & \text{if } x < x_d, \\ \mathbf{U}_r & \text{if } x > x_d, \end{cases}$$

- Solution at time  $t$ .
- Wave speed:  $a$ .

$$\mathbf{U} = \begin{cases} \mathbf{U}_l & \text{if } x < at, \\ \mathbf{U}_r & \text{if } x > at, \end{cases}$$

## Compressible hydrodynamics

$$\frac{\partial \rho}{\partial t} + \nabla \cdot (\rho \mathbf{v}) = 0 ,$$

$$\frac{\partial(\rho \mathbf{v})}{\partial t} + \nabla \cdot [\rho \mathbf{v} \otimes \mathbf{v} + p_g] = 0 ,$$

$$\frac{\partial E}{\partial t} + \nabla \cdot [(E + p_g) \mathbf{v}] = 0 ,$$

where the energy density is defined as

$$E = \frac{p_g}{\gamma - 1} + \frac{\rho v^2}{2} ,$$

# Compressible hydrodynamics

**Strictly** hyperbolic.

$$\frac{\partial \mathbf{U}}{\partial t} + \frac{\partial \mathbf{F}}{\partial x} = 0.$$

Real and **distinct** eigenvalues:

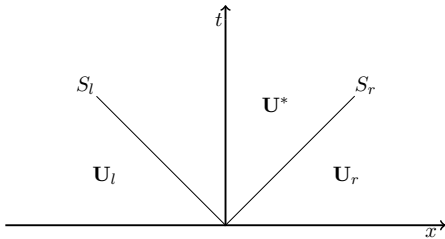
$$\lambda_3 = v_n + a : \text{rarefaction or shock}$$

$$\lambda_2 = v_n : \text{contact discontinuity}$$

$$\lambda_1 = v_n - a : \text{rarefaction or shock}$$

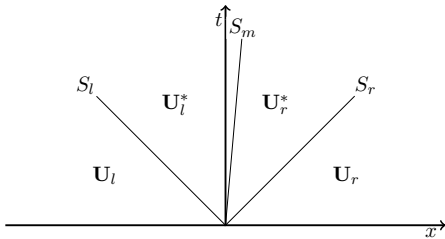
where  $a = \sqrt{\gamma p_g / \rho}$  is the speed of sound.

## HLL family of approximate Riemann solvers



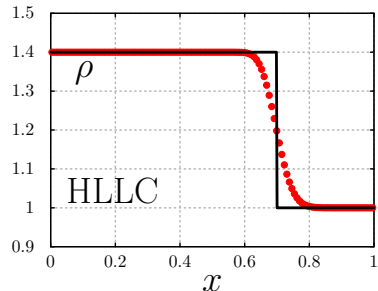
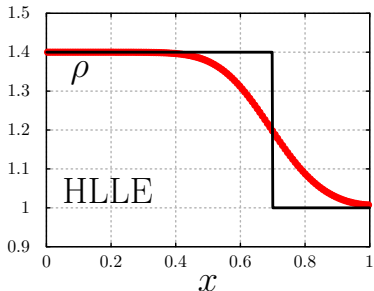
- The solver of Harten-Lax-van Leer-Einfeldt (HLLE) [3] assumes a one state solution.
- The solution approximated as weighted average of the left and right states.

## HLL family of approximate Riemann solvers



- The solver of Harten-Lax-van Leer-Einfeldt (HLLE) [3] assumes a one state solution.
- The solution approximated as weighted average of the left and right states.
- HLLC [12] (C for *contact*) restores the contact discontinuity.

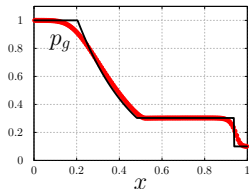
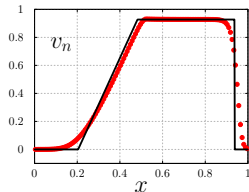
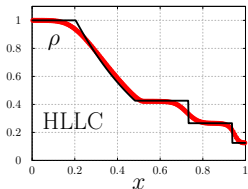
# HLL family of approximate Riemann solvers



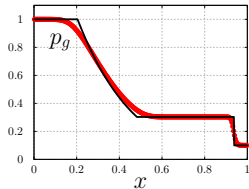
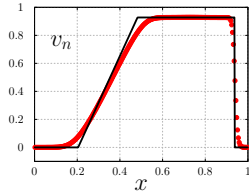
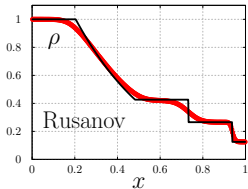
- The solver of Harten-Lax-van Leer-Einfeldt (HLLE) [3] assumes a one state solution.
- The solution approximated as weighted average of the left and right states.
- HLLC [12] (C for *contact*) restores the contact discontinuity.
- HLLC less diffuse at contact discontinuity.

# Higher order extensions

- **Total variation diminishing (TVD): Limit slope [5].**



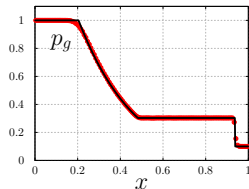
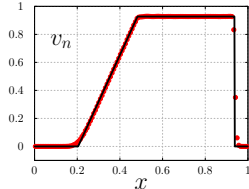
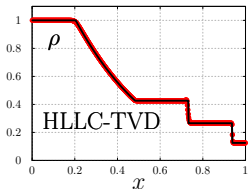
- **Flux corrected transport (FCT): Limit flux [1].**



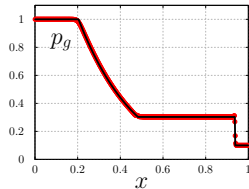
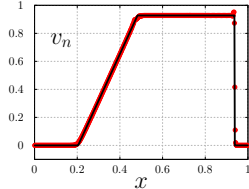
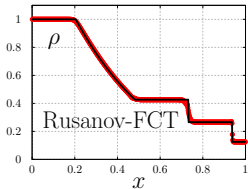
\* TVD approximation computed with Athena [11].

# Higher order extensions

- **Total variation diminishing (TVD):** Limit slope [5].



- **Flux corrected transport (FCT):** Limit flux [1].



\* TVD approximation computed with Athena [11].

## Ideal magnetohydrodynamics

$$\frac{\partial \rho}{\partial t} + \nabla \cdot (\rho \mathbf{v}) = 0 ,$$

$$\frac{\partial(\rho \mathbf{v})}{\partial t} + \nabla \cdot \left[ \rho \mathbf{v} \otimes \mathbf{v} + \left( p_g + \frac{B^2}{2} \right) \mathbf{I} - \mathbf{B} \otimes \mathbf{B} \right] = 0 ,$$

$$\frac{\partial E}{\partial t} + \nabla \cdot \left[ \left( E + p_g + \frac{B^2}{2} \right) \mathbf{v} - \mathbf{v} \cdot \mathbf{B} \otimes \mathbf{B} \right] = 0 , \text{ and}$$

$$\frac{\partial \mathbf{B}}{\partial t} + \nabla \cdot [\mathbf{v} \otimes \mathbf{B} - \mathbf{B} \otimes \mathbf{v}] = 0 ,$$

where the energy density is defined as

$$E = \frac{p_g}{\gamma - 1} + \frac{\rho v^2}{2} + \frac{B^2}{2} ,$$

# Ideal magnetohydrodynamics

**Non-strictly** hyperbolic.

$$\frac{\partial \mathbf{U}}{\partial t} + \frac{\partial \mathbf{F}}{\partial x} = 0.$$

Real, but **not** necessarily distinct eigenvalues:

$\nu_n$  : contact or tangential discontinuity (entropy),

$\nu_n \pm c_s$  : slow rarefaction or shock,

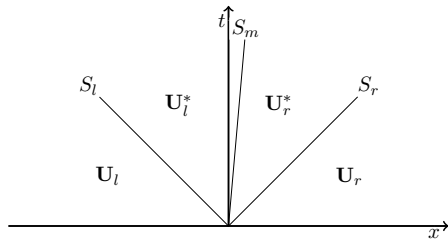
$\nu_n \pm c_a$  : rotational discontinuity (Alfvén), and

$\nu_n \pm c_f$  : fast rarefaction or shock,

$$c_{f,s}^2 = \frac{1}{2} \left[ a^2 + c_a^2 + c_t^2 \pm \sqrt{(a^2 + c_a^2 + c_t^2)^2 - 4a^2 c_a^2} \right],$$

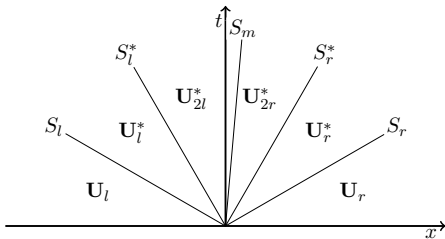
$$c_a^2 = \frac{B_n^2}{\rho}, \text{ and } c_t^2 = \frac{B_t^2}{\rho}.$$

# Extension of HLLC for MHD



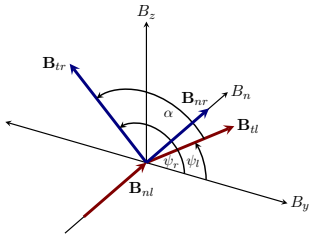
- HLLD [8] (D for *discontinuities*) extention of HLLC to MHD.

# Extension of HLLC for MHD



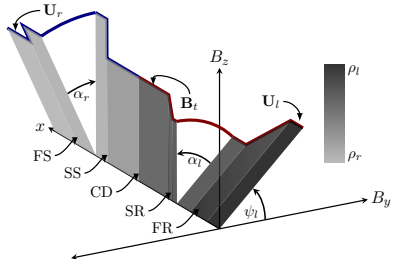
- HLLD [8] (D for *discontinuities*) extention of HLLC to MHD.
- Captures linear discontinuities: contact and rotational.

# Riemann problems of ideal MHD



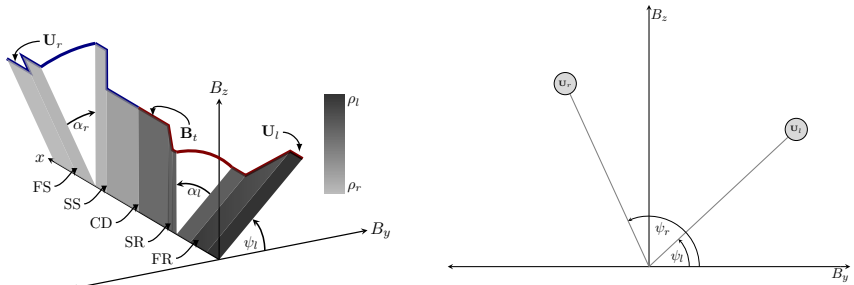
- Initial discontinuity separates two states.
- Rotation angle  $\arctan B_z/B_y$ .
- The initial twist angle  $\alpha = \psi_r - \psi_l$ .

# Riemann problems of ideal MHD



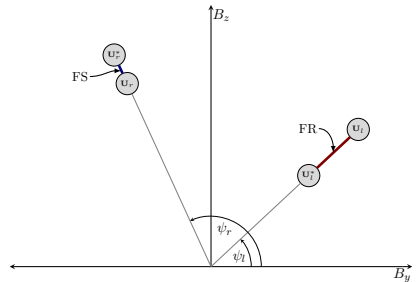
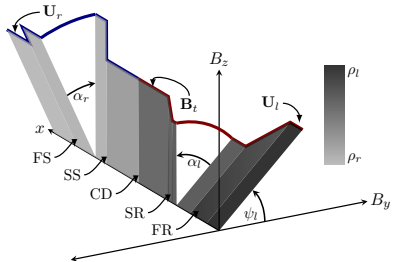
- Seven waves, eight states.

# Riemann problems of ideal MHD



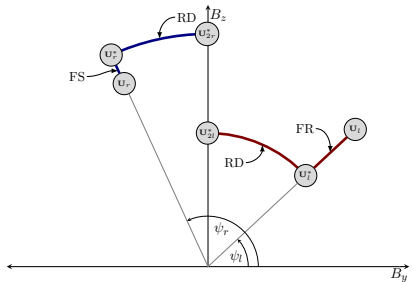
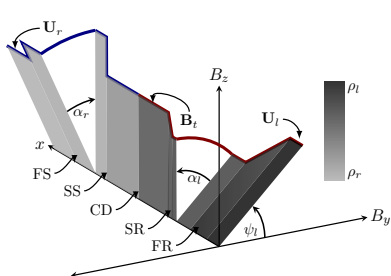
- Regular waves alter magnitude or orientation of  $B_t$ .

# Riemann problems of ideal MHD



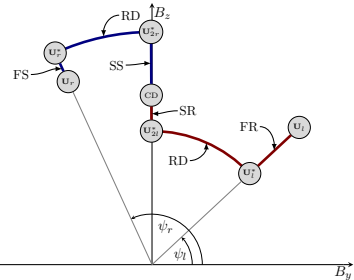
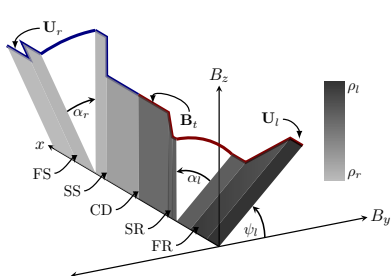
- Regular waves alter magnitude or orientation of  $B_t$ .
- Fast shock:  $B_t \uparrow$ , fast rarefaction:  $B_t \downarrow$ .

# Riemann problems of ideal MHD



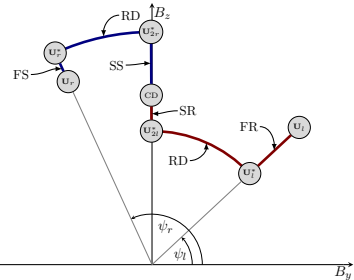
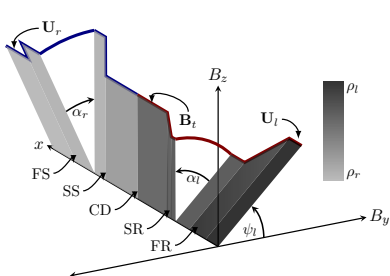
- Regular waves alter magnitude or orientation of  $B_t$ .
- Fast shock:  $B_t \uparrow$ , fast rarefaction:  $B_t \downarrow$ .
- Rotational discontinuity:  $\psi \pm \delta\psi$ .

# Riemann problems of ideal MHD



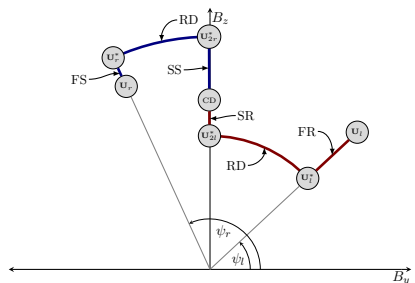
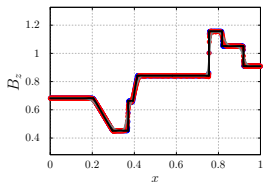
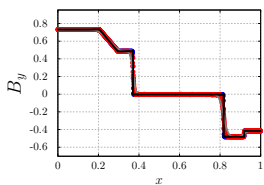
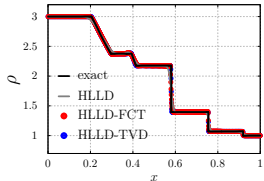
- Regular waves alter magnitude or orientation of  $B_t$ .
- Fast shock:  $B_t \uparrow$ , fast rarefaction:  $B_t \downarrow$ .
- Rotational discontinuity:  $\psi \pm \delta\psi$ .
- Slow shock:  $B_t \downarrow$ , slow rarefaction:  $B_t \uparrow$ .

# Riemann problems of ideal MHD

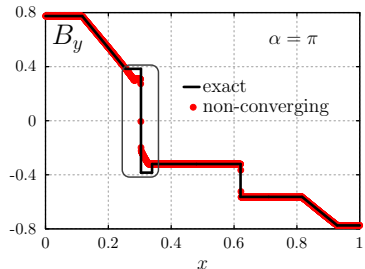
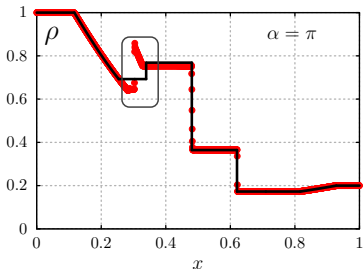


- Regular waves alter magnitude or orientation of  $B_t$ .
- Fast shock:  $B_t \uparrow$ , fast rarefaction:  $B_t \downarrow$ .
- Rotational discontinuity:  $\psi \pm \delta\psi$  .
- Slow shock:  $B_t \downarrow$ , slow rarefaction:  $B_t \uparrow$ .
- Contact discontinuity: no change.

# Riemann problems of ideal MHD

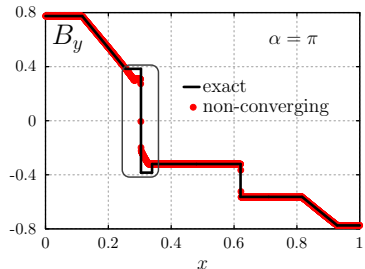
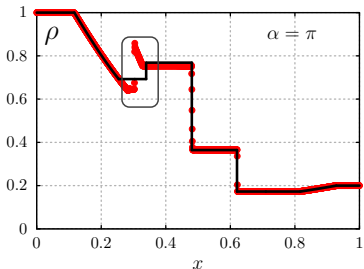


# Non-unique solutions



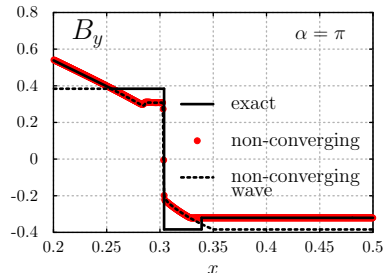
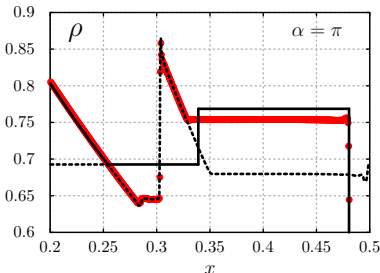
- Solutions to coplanar Riemann problems of ideal MHD are non-unique.
- At  $x = 0.303$ , rotational discontinuity  $\rightarrow$  compound wave.

# Non-unique solutions



- Solutions to coplanar Riemann problems of ideal MHD are non-unique.
- At  $x = 0.303$ , rotational discontinuity  $\rightarrow$  compound wave.
- Compound wave is composed of an intermediate shock and a slow rarefaction.
- Physical?
- Unstable for under small perturbations [7].
- Satisfies jump conditions in the coplanar case.

# Non-unique solutions



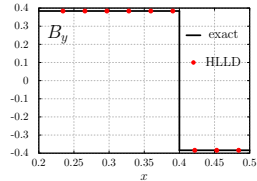
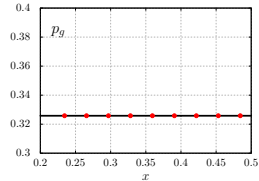
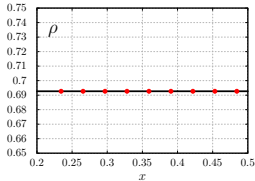
- Intermediate shock: alters magnitude and orientation of magnetic field.
- Slow compound wave: super-Alfvénic  $\rightarrow$  sub-slow.
- In shock frame upstream:  $c_a < v_n < c_f$

$$v_n = 1.0174, c_a = 0.9661, c_f = 1.1295$$

- In shock frame downstream:  $v_n < c_s, c_a$

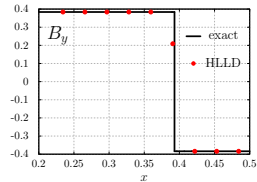
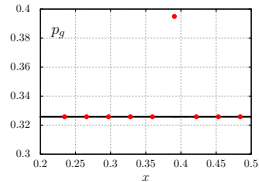
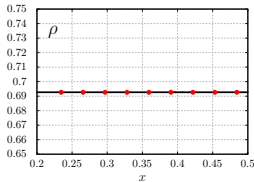
$$v_n = 0.7341, c_s = 0.8033, c_a = 0.8222$$

# Compound wave formation



- Compound waves are a product of numerical diffusion.

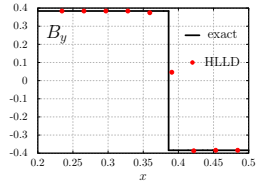
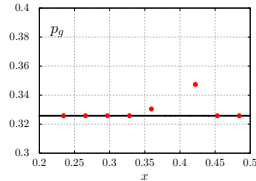
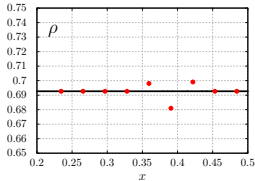
# Compound wave formation



- Compound waves are a product of numerical diffusion.
- Decrease  $B_t \rightarrow$  increase  $p_g$

$$p_g = (\gamma - 1) \left( E - \frac{\rho v^2}{2} - \frac{B^2}{2} \right)$$

# Compound wave formation

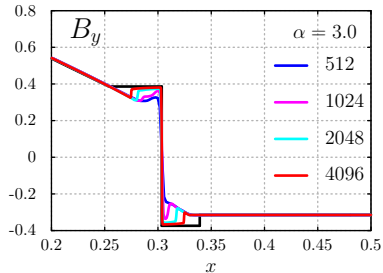
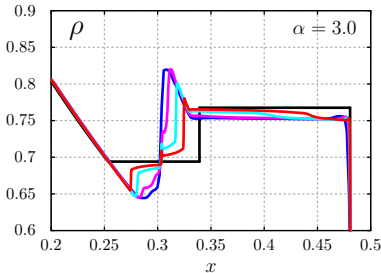


- Compound waves are a product of numerical diffusion.
- Decrease  $B_t \rightarrow$  increase  $p_g$

$$p_g = (\gamma - 1) \left( E - \frac{\rho v^2}{2} - \frac{B^2}{2} \right)$$

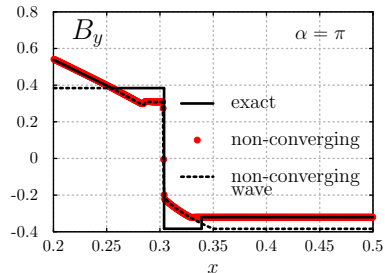
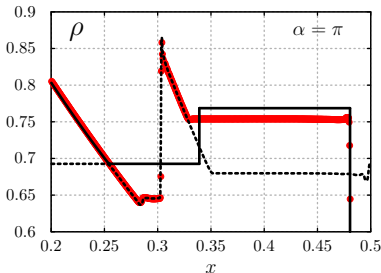
- Increase  $p_g \rightarrow$  compound wave.

# Pseudo-convergence



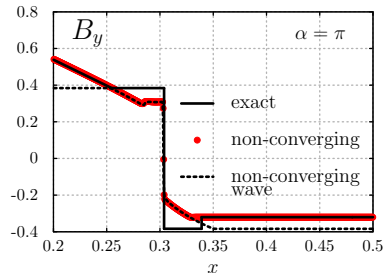
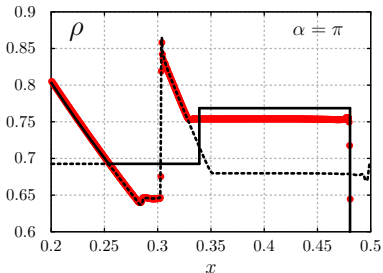
- $\alpha < \pi$ , compound waves at lower resolutions.
- Pseudo-convergence: rotational discontinuity at higher resolutions [13].
- Transition between 1024 and 2048 grid points.
- $\alpha \rightarrow \pi$ , grid resolution increases.
- $\pi = \alpha$ , compound wave at all resolutions.

# Compound Wave modification



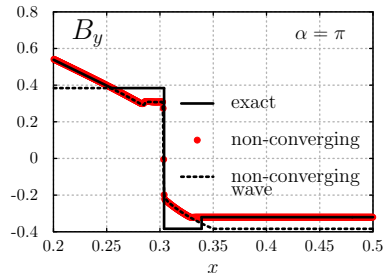
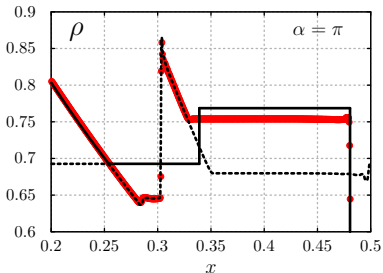
- Compound waves are product of numerical diffusion for near coplanar problems.
- Reduce diffusion to recover correct solution. How?

# Compound Wave modification



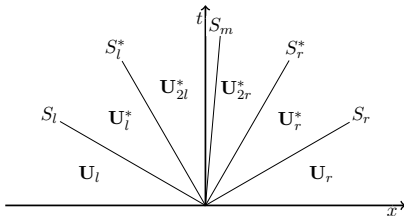
- Compound waves are product of numerical diffusion for near coplanar problems.
- Reduce diffusion to recover correct solution. How?
- $\rho$  and  $B_t$  should remain constant across the rotational discontinuity  $x = 0.303$ .

# Compound Wave modification

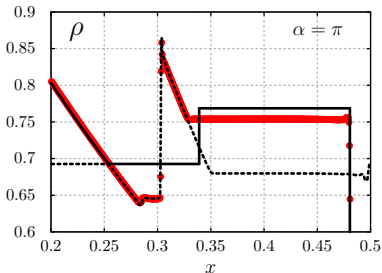


- Compound waves are product of numerical diffusion for near coplanar problems.
- Reduce diffusion to recover correct solution. How?
- $\rho$  and  $B_t$  should remain constant across the rotational discontinuity  $x = 0.303$ .
- Limit flux associated with the compound wave.

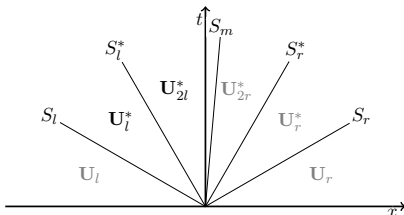
# Compound Wave modification



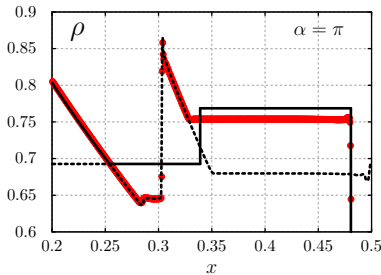
- Use HLLD to approximate intermediate states upstream and downstream of rotational discontinuity, i.e.,  $\mathbf{U}_l^*$  and  $\mathbf{U}_{2l}^*$ .



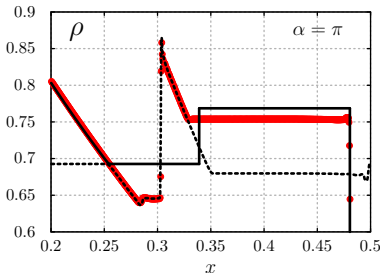
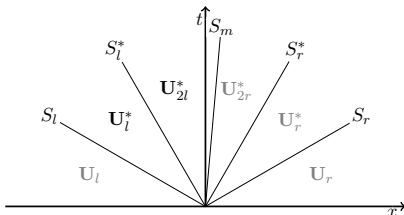
# Compound Wave modification



- Use HLLD to approximate intermediate states upstream and downstream of rotational discontinuity, i.e.,  $\mathbf{U}_l^*$  and  $\mathbf{U}_{2l}^*$ .
- Calculate flux  $\mathbf{F}^c$  between  $\mathbf{U}_l^*$  and  $\mathbf{U}_{2l}^*$  responsible for formation of the compound wave.

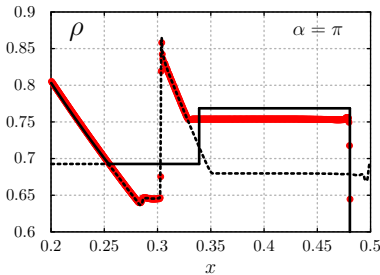
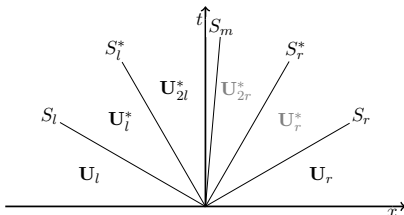


# Compound Wave modification



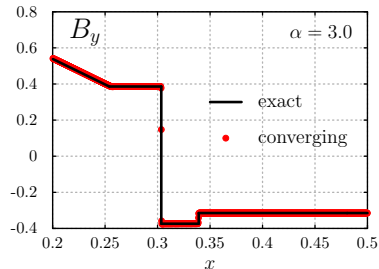
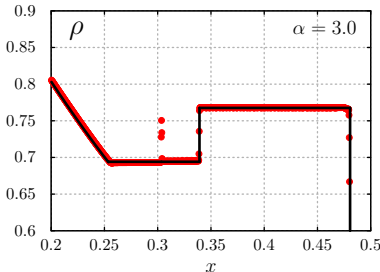
- Use HLLD to approximate intermediate states upstream and downstream of rotational discontinuity, i.e.,  $\mathbf{U}_l^*$  and  $\mathbf{U}_{2l}^*$ .
- Calculate flux  $\mathbf{F}^c$  between  $\mathbf{U}_l^*$  and  $\mathbf{U}_{2l}^*$  responsible for formation of the compound wave.
- Reduce the contribution of  $\mathbf{F}^c = \mathbf{F}_{hlld}(\mathbf{U}_l^*, \mathbf{U}_{l/2}^*)$  to the total flux.

# Compound Wave modification



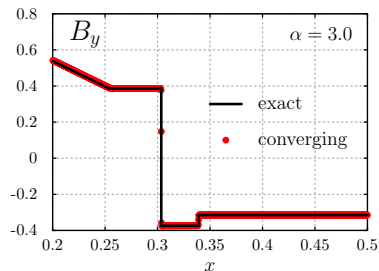
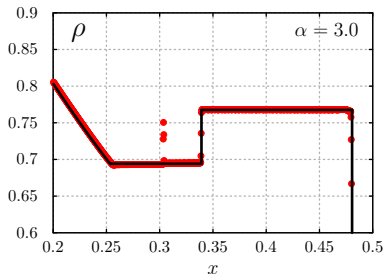
- Use HLLD to approximate intermediate states upstream and downstream of rotational discontinuity, i.e.,  $\mathbf{U}_l^*$  and  $\mathbf{U}_{2l}^*$ .
- Calculate flux  $\mathbf{F}^c$  between  $\mathbf{U}_l^*$  and  $\mathbf{U}_{2l}^*$  responsible for formation of the compound wave.
- Reduce the contribution of  $\mathbf{F}^c = \mathbf{F}_{hlld}(\mathbf{U}_l^*, \mathbf{U}_{l/2})$  to the total flux.
- $\mathbf{F}_{cwm} = \mathbf{F}_{hlld}(\mathbf{U}_l, \mathbf{U}_r) - A\mathbf{F}^c$ , where  $A < 0.5$ .

# CWM Results



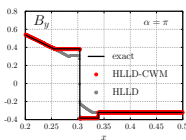
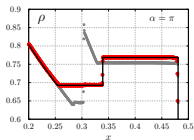
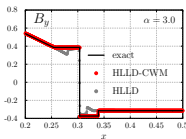
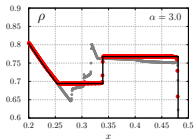
- CWM recovers the correct solution upstream and downstream of rotational discontinuity.
- Transition across rotational discontinuity is unresolved.
- Resolve it?

# CWM Results



- CWM recovers the correct solution upstream and downstream of rotational discontinuity.
- Transition across rotational discontinuity is unresolved.
- Resolve it?
- Simple but non-conservative.

# CWM Resolving the transition



- Jump conditions in Lagrangian mass coordinates,  $V = 1/\rho$ ,  $W$  is wave speed.
- Brackets denote difference across discontinuity.

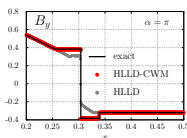
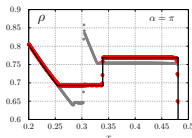
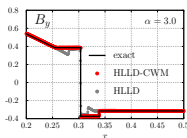
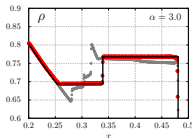
$$W[V] = -[v_n],$$

$$W[v_n] = -[P - B_n^2],$$

$$W[\mathbf{v}_t] = -B_n[\mathbf{B}_t],$$

$$W[V\mathbf{B}_t] = -B_n[\mathbf{v}_t],$$

# CWM Resolving the transition



- Across rotational discontinuity

$$[V] = 0,$$

$$[v_n] = 0,$$

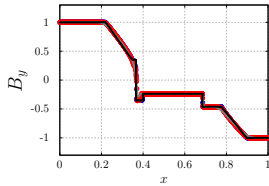
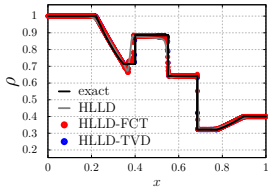
$$[p_g] = 0,$$

$$[B_t] = 0,$$

$$W[\mathbf{v}_t] = -B_n[\mathbf{B}_t],$$

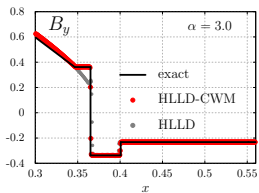
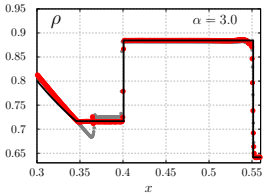
- $W = \sqrt{\rho}B_n$  is Lagrangian speed of linear wave.

# Results



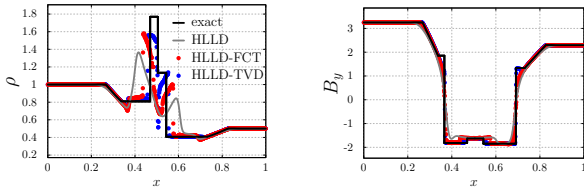
- Near coplanar initial conditions.
- Fast compound wave at  $x = 0.365$

# Results



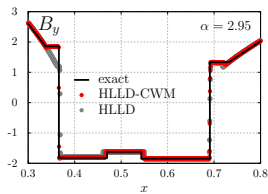
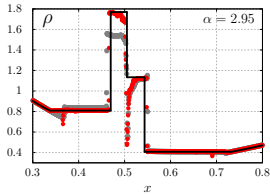
- Near coplanar initial conditions.
- Fast compound wave at  $x = 0.365$
- Small deviation for weak intermediate shocks.

# Results



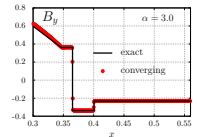
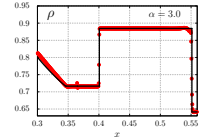
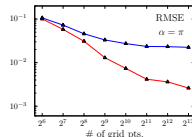
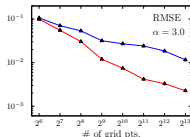
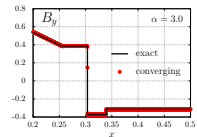
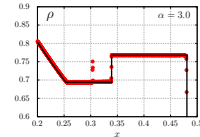
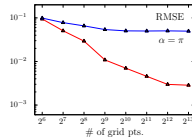
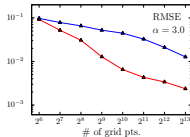
- Non-planar initial conditions.
- Fast compound waves at  $x = 0.366$  and  $x = 0.691$

# Results



- Non-planar initial conditions.
- Fast compound waves at  $x = 0.366$  and  $x = 0.691$
- Small deviation for weak intermediate shocks.

# Error analysis

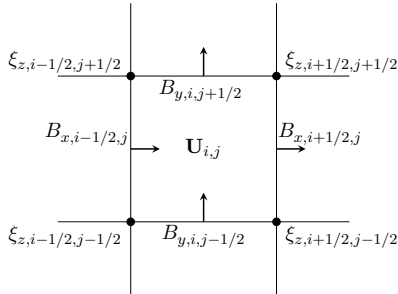


- Error calculation without applying the correction at the rotational discontinuity.
- Without CWM, the compound wave starts to break apart between  $2^{10}$  and  $2^{11}$ .
- CWM produces convergence at low grid resolutions.

# Higher dimensions

Maintaining  $\nabla \cdot \mathbf{B} = 0$  with constrained transport [4].

- Staggered grid.
- Hydrodynamical variables at cell centers.
- Magnetic field at interface.
- $\mathbf{E} = -\mathbf{v} \times \mathbf{B}$  at corners.
- Denote z-component of the emf as  $\xi_z$ .



Finite area integration of interface  $\mathbf{B}$

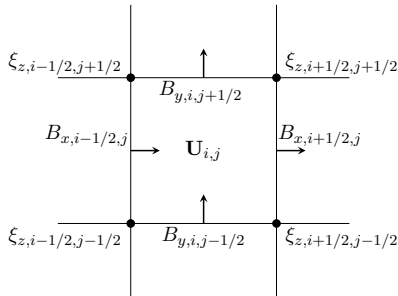
$$B_{x,i+1/2,j}^{n+1} = B_{x,i+1/2,j}^n - \frac{\delta t}{\delta y} (\xi_{z,i+1/2,j+1/2} - \xi_{z,i+1/2,j-1/2})$$

$$B_{y,i,j+1/2}^{n+1} = B_{y,i,j+1/2}^n + \frac{\delta t}{\delta x} (\xi_{z,i+1/2,j+1/2} - \xi_{z,i-1/2,j-1/2})$$

# Higher dimensions

Maintaining  $\nabla \cdot \mathbf{B} = 0$  with constrained transport [4].

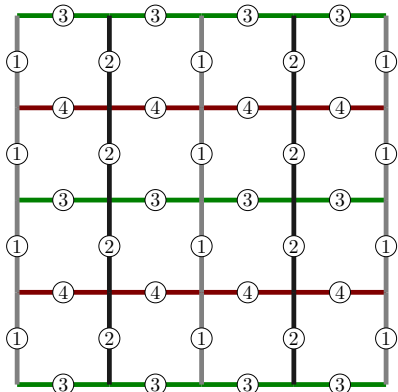
- Staggered grid.
- Hydrodynamical variables at cell centers.
- Magnetic field at interface.
- $\mathbf{E} = -\mathbf{v} \times \mathbf{B}$  at corners.
- Denote z-component of the emf as  $\xi_z$ .



Due to perfect cancellation, the numerical divergence in the cell remains zero to machine precision.

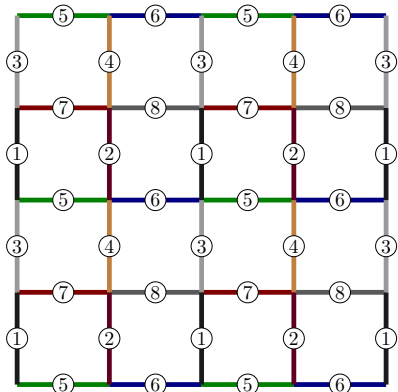
$$(\nabla \cdot \mathbf{B})_{i,j} = \frac{1}{\delta x} (B_{x,i+1/2,j} - B_{x,i-1/2,j}) + \frac{1}{\delta y} (B_{y,i,j+1/2} - B_{y,i,j-1/2})$$

# Shared memory parallelism



- Faces must be grouped by color to avoid memory contention.
- Loop over the faces becomes loop over the colors.

# Shared memory parallelism



- Faces must be grouped by color to avoid memory contention.
- Loop over the faces becomes loop over the colors.
- Constrained transport, faces and edges must be colored.

## Efficient algorithms

```
thrust::device_vector<float> x(n);    // independent
                                         variable
thrust::device_vector<float> y(n);    // y = f(x)
thrust::device_vector<float> z(n);    // z = g(y)

// compute y = f(x)
thrust::transform(x.begin(),x.end(),y.begin(),f());

// compute z = g(y)
thrust::transform(y.begin(),y.end(),z.begin(),g());
```

- Function composition [6].
- $3n$  floats,  $2n$  reads,  $2n$  writes, and uses  $n$  temporary floats.

# Efficient algorithms

```
thrust::device_vector<float> x(n);    // independent
                                         variable
thrust::device_vector<float> z(n);    // z = g(y) = g(
                                         f(x))

// compute z = g(f(x))
thrust::transform(make_transform_iterator(x.begin(),
                                         f()),
                  make_transform_iterator(x.end(),
                                         () ),
                  z.begin(),
                  g());
```

- Function composition [6].
- $2n$  floats,  $n$  reads,  $n$  writes, and no temporary storage.

# Memory access

```
struct
    conservative_variables{
        float density;
        float momentum_x;
        float energy;
    }

    conservative_variables
    *state; // AoS

    state[i].density =
        some_number;
    state[i].momentum_x =
        another_number;
    state[i].energy =
        one_more_number;
```

```
struct
    conservative_variables{
        float *density;
        float *momentum_x;
        float *energy;
    }

    conservative_variables
    state; // SoA

    state.density[i] =
        some_number;
    state.momentum_x[i] =
        another_number;
    state.energy[i] =
        one_more_number;
```

- Memory coalescing occurs when multiple memory addresses are accessed with a single transaction.
- Memory does not coalesce with AoS (left).
- Memory does coalesce with SoA (right).

## Memory access

```
thrust::device_vector<primitive_variables>
    primitive_state(n); // AoS
thrust::device_vector<conservative_variables>
    conservative_state(n); // AoS
thrust::transform_n(primitive_state.begin(),
                   primitive_state.size(),
                   conservative_state.begin(),
                   convert_primitive_to_conservative(
                       gamma));
```

- Converting from primitive variables  $(\rho, v_x, p_g)$  to conservative variables  $(\rho, \rho v_x, en)$ .
- No coalescing.

## Memory access

```
thrust::device_vector<float> d(n), vx(n), pg(n);
thrust::device_vector<float> mx(n), en(n);
thrust::transform_n(
    thrust::make_zip_operator(
        make_tuple(d.begin(),
                   vx.begin(),
                   pg.begin())),
    n,
    thrust::make_zip_operator(
        make_tuple(d.begin(),
                   mx.begin(),
                   en.begin())),
    convert_primitive_to_conservative(gamma));
```

- Converting from primitive variables ( $\rho, v_x, p_g$ ) to conservative variables ( $\rho, \rho v_x, en$ ).
- Arrays can be combined on the fly with a `zip_operator` to achieve coalescing.

# Performance Comparison

Performance comparison for Orszag-Tang [9] test.

grid size	cells/second (GPU)	cells/second (CPU)	ratio
$64 \times 64$	$4.1894 \times 10^6$	$7.3955 \times 10^5$	5
$128 \times 128$	$1.6540 \times 10^7$	$7.5060 \times 10^5$	22
$256 \times 256$	$4.4497 \times 10^7$	$7.3155 \times 10^5$	60
$512 \times 512$	$6.3286 \times 10^7$	$7.9437 \times 10^5$	79
$1024 \times 1024$	$7.2134 \times 10^7$	$8.3354 \times 10^5$	86

- Dell Precision 7500 workstation with a (Dual CPU)
- CPU Intel Xeon E5645 @ 2.40 Ghz.
- GPU GeForce GTX TITAN with a memory bandwidth of 288.4 GB/sec and 2688 CUDA cores.
- Almost a factor of three increase of speed ratio from  $128 \times 128$  to  $256 \times 256$ .

# Conclusion

- Compound wave modification:
  - ▶ Produces rotational discontinuity for coplanar problems.
  - ▶ Removes pseudo-convergence for near coplanar problems.
  - ▶ Does not require exact solver.
  - ▶ FAST! HLLD intermediate states are already calculated.
  - ▶ Produces the correct result when other numerical inaccuracies are present.
- Released\* a nonlinear solver for ideal MHD.
- Released\* a high-order multi-dimensional fluid solver.
  - ▶ General geometry on unstructured grids.
  - ▶ Capable of shared memory parallelism on GPU and CPU.
  - ▶ Can be used as blueprint or benchmark by anyone in computational physics and space weather communities wishing to increase performance.

# Bibliography I

- [1] J. P. Boris and D. L. Book. “Flux-Corrected Transport I. SHASTA, A Fluid Transport Algorithm That Works”. In: *J. Comp. Phys.* 11 (1973), pp. 38–69.
- [2] H. de Sterck, B. C. Low, and S. Poedts. “Complex magnetohydrodynamic bow shock topology in field-aligned low- $\beta$  flow around a perfectly conducting cylinder”. In: *Physics of Plasmas* 5 (Nov. 1998), pp. 4015–4027.
- [3] B. Einfeldt. “On Godunov-Type Methods for Gas Dynamics”. In: *SIAM J. Numer. Anal.* 25 (1988), pp. 294–318.
- [4] C. R. Evans and J. F. Hawley. “Simulation of magnetohydrodynamic flows - A constrained transport method”. In: *ApJ* 332 (Sept. 1988), pp. 659–677.

## Bibliography II

- [5] A. Harten. "High resolution schemes for hyperbolic conservation laws". In: *J. Comp. Phys.* 49 (1983), pp. 357–393.
- [6] Jared Hoberock and Nathan Bell. *Thrust: A Parallel Template Library*. Version 1.7.0. 2010. URL: <http://thrust.github.io/>.
- [7] L. D. Landau, E. M. Lifshitz, and L. P. Pitaevskii. *Electrodynamics of continuous media*. 3rd. 1984.
- [8] T. Miyoshi and K. Kusano. "A multi-state HLL approximate Riemann solver for ideal MHD". In: *J. Comp. Phys.* 208 (May 2005), pp. 315–344.
- [9] S. A. Orszag and C.-M. Tang. "Small-scale structure of two-dimensional magnetohydrodynamic turbulence". In: *Journal of Fluid Mechanics* 90 (Jan. 1979), pp. 129–143.

## Bibliography III

- [10] *Spasce Weather.* [http://now.uiowa.edu/files/now.uiowa.edu/styles/prim\\_horizontal\\_640/public/sun-earth-640.jpg?itok=ESKvx0GJ](http://now.uiowa.edu/files/now.uiowa.edu/styles/prim_horizontal_640/public/sun-earth-640.jpg?itok=ESKvx0GJ).
- [11] J. Stone, T. Gardner, and P. Teuben. *Athena MHD Code Project*. <https://trac.princeton.edu/Athena/>. Dec. 2010.
- [12] E. F. Toro, M. Spruce, and W. Speares. “Restoration of the contact surface in the HLL-Riemann solver”. In: *Shock Waves* 4 (Mar. 1994), pp. 25–34.
- [13] M. Torrilhon. “Non-uniform convergence of finite volume schemes for Riemann problems of ideal magnetohydrodynamics”. In: *J. Comp. Phys.* 192 (Nov. 2003), pp. 73–94.